F192628-73-C-0006, the National Science Foundation under Grant No. GA35823, and the U. S. Atomic Energy Commission under Contract No. AT(11-1)3063.

[1]D. Adler and J. Feinleib, Phys. Rev. B 2, 3112 (197 (1970).

[2]T. M. Wilson, Int. J. Quantum Chem., Symp. 1970, 757.

[3]K. H. Johnson, R. P. Messmer, and J. W. D. Connolly, Solid State Commun. 12, 313 (1973); R. P. Messmer, C. W. Tucker, Jr., and K. H. Johnson, Surface Sci. 42, 341 (1974).

[4]B. Koiller and L. M. Falicov, J. Phys. C: Proc. Phys. Soc., London 7, 299 (1974).

[5]G. K. Wertheim and S. Hüfner, Phys. Rev. Lett. 28, 1028 (1972).

[6]G. K. Wertheim, H. J. Guggenheim, and S. Hüfner, Phys. Rev. Lett. 30, 1050 (1973).

[7]K. S. Kim, Chem. Phys. Lett. 26, 234 (1974).

[8]S. Sugano, Y. Tanabe, and H. Kamimura, *Multiplets of Transition Metal Ions in Crystals* (Academic, New York, 1970).

[9]R. J. Powell and W. E. Spicer, Phys. Rev. B 2, 2182 (1970).

[10]D. E. Eastman, W. D. Grobman, J. L. Freeouf, and M. Erbudak, Phys. Rev. B 9, 3473 (1974).

[11]Cr_2O_3 was prepared by evaporating a Cr film and oxidizing a thick surface layer to Cr_2O_3 at room temperature. Spectra for Cr_2O_3 were measured using He I (21.2 eV) and He II (40.8 eV) radiation.

[12]D. E. Eastman and M. Kuznietz, Phys. Rev. Lett. 26, 846 (1971).

[13]A. Goldmann, J. Tejeda, N. J. Shevchik, and M. Cardona, Phys. Rev. B 10, 4388 (1974).

[14]This factorization is only approximate, of course, and we ignore certain p-d and s-d hybridization effects as well as possible $\hbar\omega$-dependent intensities for different p and d orbitals. We expect this partial state decomposition to be approximately valid for materials such as the transition-metal oxides.

[15]Previously (Ref. 6), transition intensities were taken to be proportional to the initial-state orbital degeneracy.

[16]This description is only approximate for at least two reasons: (1) The ratio B/C is apparently different from that used by Sugano for the ground state and this may modify his calculated energies; (2) configuration interaction between many-electron wave functions with the same $S\Gamma$ representation can alter relative intensities. However, the observed agreement (Fig. 2) suggests that the assumed model is a good first approximation.

[17]*Ab initio* calculations by P. Bagus (to be published) for ground state and ionized Ni in NiO imply $B^{3+}/B^{2+} \simeq 0.67$, consistent with our present results.

[18]Crystal-field parameters Dq appropriate for a divalent ion (Ref. 8) were used; overall widths were virtually unchanged (but e_g levels shifted slightly) by using a larger (e.g., 2.5 valent) Dq.

Surface Photoelectric Effect and Orbital Symmetry: Evidence for Anomalous Dielectric Properties

J. E. Rowe
Bell Laboratories, Murray Hill, New Jersey 07974
(Received 23 September 1974)

Ultraviolet photoelectron spectra using He I resonance radiation and Ge(111) surfaces have been measured for both bonding and nonbonding orbitals. In all cases the partial photocurrent from a specific orbital is considerably enhanced for the macroscopic electric field normal to the surface independent of the orbital symmetry. This is interpreted in terms of an anomalous enhancement of the dielectric response due to surface polarization charge within the short electron escape depth ($\lambda_e \lesssim 10$ Å) at these energies.

The role of the surface in photoemission from a solid (i.e., the surface photoelectric effect) is an old topic which has been studied both experimentally[1] and theoretically[2] for more than four decades. Most experiments have concerned only the total yield which displays a strong vectorial photoeffect at low photon energy $\hbar\omega$ near threshold. Recent work has tended to concentrate on free-electron metals[3,4] but even for these materials the detailed mechanism of optical excitation is far from being completely understood[5] since both surface-plasmon effects and direct excitation are possible for $\hbar\omega \leq \hbar\omega_s$, the surface-plasmon energy. In contrast, high-energy photoemission ($\hbar\omega > \hbar\omega_p$) is expected[4] to exhibit a negligible surface photoeffect with optical selection rules determined by the symmetry properties of the photoelectron wave functions.[6-8] This paper reports the first systematic measurement of high-energy photoelectron energy spectra ($\hbar\omega > \hbar\omega_p$) as a function of angle of incidence for both bonding and nonbonding orbitals. The bonding orbitals

are directed either perpendicular or nearly parallel to the surface and the nonbonding orbitals have approximately isotropic angular symmetry. In all cases the partial photocurrent from a specific orbital shows a strong enhancement for z-polarized photons with the z axis being normal to the surface. This enhanced photocurrent is 3–4 times greater than the signal predicted from the macroscopic optical fields[4,7] and is in qualitative agreement with recent theoretical calculations of Kliewer.[9]

The Ge(111) surface was chosen for the present measurements since it satisfies the criterion of free-electron–like optical properties in the far ultraviolet, $\hbar\omega = 10$–25 eV, as well as the possibility of localized bonding effects due to directed tetrahedral covalent bonds in the bulk, to intrinsic surface states, and to chemisorption bonds. At $\hbar\omega = 21.2$ eV the photoelectron escape length is in the range $\lambda_e \sim 4$–10 Å, so that optical transitions for both surface and bulk states are determined by the photon intensity near (~ 10 Å) the surface. The germanium (111) samples were moderately doped ($p \sim 10^{15}$ cm^{-3}) and were cleaned by Ar^+-ion sputter etching and annealing at 1000°K which gave a clear 2×8 low-energy electron diffraction (LEED) pattern. The multiple-technique ultrahigh-vacuum chamber has been previously described[10,11] and has a base pressure of $p \lesssim 5 \times 10^{-11}$ Torr. The working pressure of active gases (mainly H_2, CH_3, and CO) was maintained below 2×10^{-10} Torr (measured on a nude Bayard-Alpert gauge) by the high pumping speed ($\sim 2 \times 10^4$ l/sec) of a liquid-nitrogen titanium-sublimation pump. Auger-electron spectroscopy was used to monitor surface impurities which were estimated to be less than 0.05 monolayers. Ultraviolet-photoelectron-spectroscopy (UPS) measurements were performed with a resonance lamp with a double-pass cylindrical-mirror analyzer (CMA) operating in the retard mode to give a constant electron-energy resolution of 0.2 eV. The CMA and electron pulse-counting electronics were controlled by a PDP-8/L minicomputer which was used for on-line signal averaging as well as for data reduction.

The clean Ge(111) 2×8 LEED pattern was changed to 1×1 by hydrogen exposures of 2×10^{-5} Torr-sec in the presence of a $1 \times 3 \times 0.002$ cm^3 tungsten ribbon heated to 2500°K to produce atomic hydrogen which rapidly chemisorbed.[10,11] An alternate 1×1 symmetry surface was prepared by evaporating Cd on the clean Ge 2×8 surface. The UPS measurements discussed below were performed either on the ordered 2×8 clean Ge(111) surface, on the 1×1 atomic-hydrogen-covered surface, on the 1×1 cadmium-covered surface, or on the disordered surface obtained by room-temperature Ar^+ bombardment to saturation concentrations of Ar ions implanted.

The photon beam was held fixed at an angle of 70° with respect to the CMA axis. The angle of incidence θ_i, with respect to the surface normal $\hat{n}$, was varied by rotating the sample about the CMA axis as shown in Fig. 1. Figure 1(a) shows the sample position for $\theta_i = 28°$ with the CMA axis in the plane of incidence. The oblique mounting of the sample allows the electron aperture cone of the CMA to accept a range of emission angles from normal emergence to grazing emergence. This minimizes effects of the photoelectron angular distribution. The photoelectron energy spec-

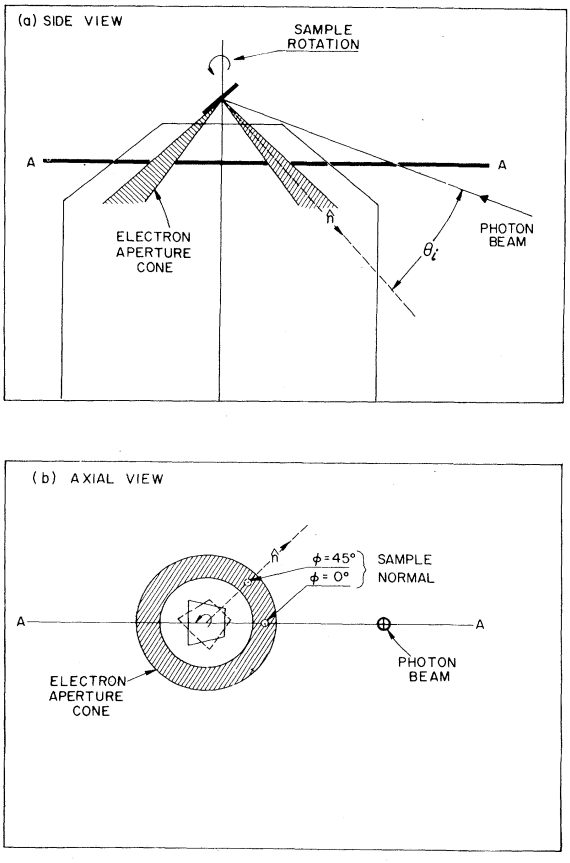

FIG. 1. Experimental geometry for varying the angle of incidence θ_i of the photon beam using a CMA to detect the photoelectrons. The photon beam is fixed with respect to the CMA axis. The sample normal $\hat{n}$ is oriented at 42° from the CMA axis and describes a circular arc as the sample is rotated through an angle φ, which is a nonlinear function of θ_i.

tra were nearly the same in this geometry as earlier results taken with the surface normal $\hat{n}$ aligned on the CMA axis[10]; thus angular-emission effects are not important in these measurements. Figure 1(b) shows an axial projection of the sample, the CMA acceptance cone, the photon beam, and two orientations of the sample normal corresponding to $\theta_i = 28°$ for $\varphi = 0°$ and $\theta_i = 42°$ for $\varphi = 45°$. Because of cylindrical symmetry the electron angular distribution is kept fixed as the sample is rotated. The sample positioning and rotation was accomplished by a modified Varian precision manipulator, model 981-0523.

Typical experimental results for $\hbar\omega = 21.2$ eV and for eight values of θ_i are shown in Fig. 2 for the Ge(111) surface with saturation coverage of atomic hydrogen having a 1×1 LEED pattern with

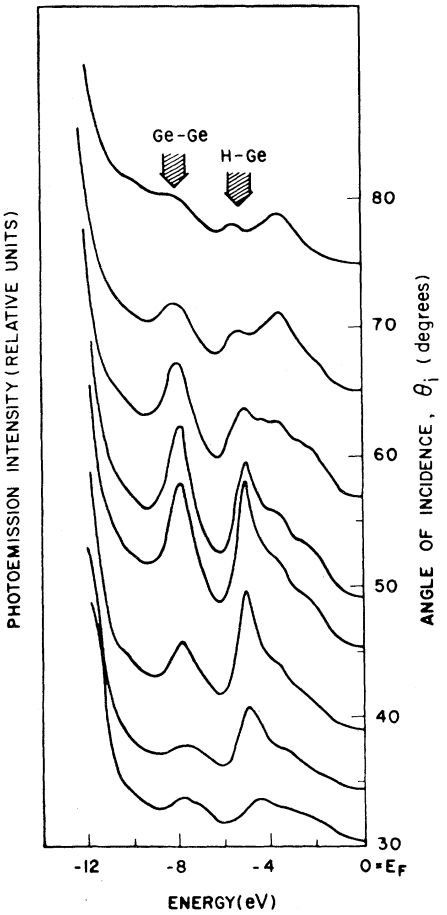

FIG. 2. Photoelectron energy distribution spectra for the Ge(111) surface with adsorbed atomic hydrogen having a 1×1 LEED pattern. The peaks near −5.0 and −7.8 eV are due to H-Ge and Ge-Ge bonds, respectively, and both have maximum intensity for angle of incidence $\theta_i \approx 45$–$55°$.

low background intensity. The Fermi-energy reference ($E_F = 0$) was determined by UPS from the tantalum sample holder. The peak at -5.0 ± 0.2 eV has intensity proportional to the hydrogen exposure at low coverages. The atomic hydrogen is probably bonded in the dangling-bond tetrahedral position normal to the surface similar to previous results for silicon (111) and (100) surfaces.[11] The peak at -7.8 ± 0.2 eV is due to Ge-Ge bonds and is predominately a bulk band-structure effect[12] but for the (111) surface three of the four tetrahedral bonds are nearly parallel to the surface. The experimental intensity is nearly zero at the Fermi energy E_F, but the vertical positions have been shifted according to the angle of incidence θ_i. The main feature of both these UPS peaks is the maximum intensity which occurs for $\theta_i \approx 45°$–$55°$.

The areas under both H-Ge and Ge-Ge peaks were computed by assuming either a constant background intensity or a linear background in the spectra of Fig. 2. Both approximations gave similar results although the peak-intensity angle θ_{max} shifted by $\lesssim 4°$ which is within the range of experimental uncertainty of $\pm 4°$. These results are consistent with a strong preference for the E_z component of the photon field since only the z component displays a maximum with increasing θ_i. The macroscopic photon field intensity just inside the surface (i.e., at $Z = Z_0^-$ in the notation of Ref. 4) as a function of θ_i is shown in Fig. 3(a) for both the total intensity $\langle E_{tot}^2 \rangle = \langle E_x^2 \rangle + \langle E_y^2 \rangle + \langle E_z^2 \rangle$ and the z component $\langle E_z^2 \rangle$. A unit intensity of unpolarized light was assumed incident on the germanium surface and Maxwell's equations were used to calculate the net intensity after reflection and transmission at the surface boundary.[13] The experimental UPS peak areas are shown in Fig. 3(b) for the H-Ge orbital resonance, for the Ge-Ge resonance, for the nonbonding Ar $3p$-orbital resonance at -8.5 eV due to implanted argon prior to annealing, and for the nonbonding $d_{5/2}$ orbital of a monolayer of cadmium adsorbed with a 1×1 LEED pattern. The zero position of each curve has been shifted vertically for clarity and the maximum intensity has been normalized to 1.0 in relative units. The detailed shape of each curve is different because of orbital symmetry differences and experimental uncertainties but to first approximation the maxima are very similar and occur near θ_i corresponding to a maximum[14] in $\langle E_z^2 \rangle$. Note that Fig. 3(a) predicts that even at its maximum $\langle E_z^2 \rangle$ is only 35% of the total intensity while the experi-

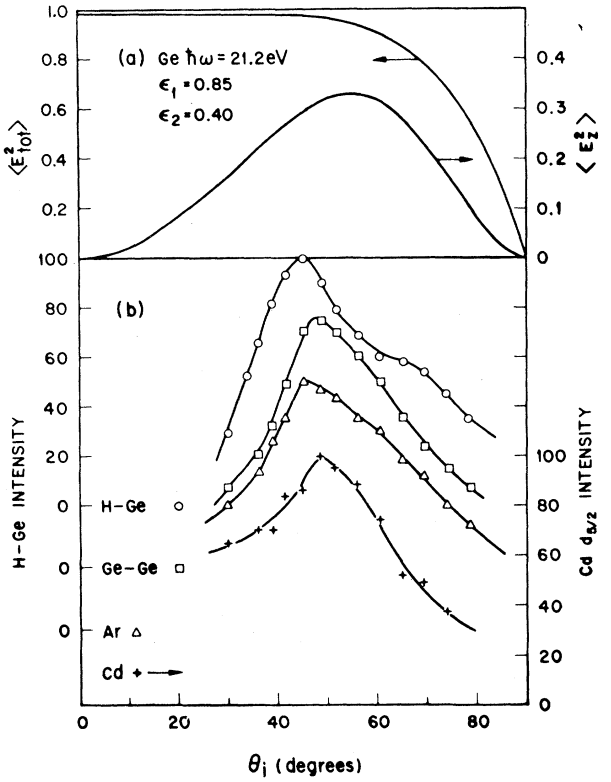

FIG. 3. (a) Macroscopic photon field intensity as a function of angle of incidence for the total field and for the z component normal to the surface. (b) Relative photoelectron peak areas as a function of angle of incidence for four different orbitals at Ge(111) surfaces. Note that all orbitals show a maximum intensity in the range $\theta_i \approx 45$–$55°$. The zero of each curve is offset for clarity.

mental peaks increase by a factor of 3–4 at maximum compared with $\theta_i = 28°$. Very similar results for both adsorbate orbitals and substrate orbitals have been obtained on Si(111) and Cd(10$\bar{1}$0) surfaces. For Cd surfaces the maximum occurred for $\theta_i \approx 65°$–$75°$ because of a difference in optical constants. Further discussion will be postponed to a later paper.

In order to explain this strong z-polarization selection rule using the usual theoretical models,[4,6-8] one must assume that the potential has a much stronger potential gradient component normal to the surface than parallel to the surface, i.e., a free-electron–like potential. This is essentially the interpretation used by Feuerbacher and Fitton for their measurements of W(100) at fixed $\theta_i = 60°$ using polarized 10.2-eV photons[15] and may be a reasonable approximation for metals. However, it seems unlikely that this is the case for semiconductors because of the directional covalent bonds which cause strong variations of the surface potential parallel to the surface, as well as variations perpendicular to the surface.[16] In Ref. 4 the divergence of the photon field is also shown to be essential for a proper treatment of photoemission from aluminum films. However, at higher frequencies, $\omega > \omega_p$, this term is much less important.[4] Two difficulties arise when the optical matrix element

$$M_{if} = (e/2mc)\langle f|\vec{A}\cdot\vec{p}+\vec{p}\cdot\vec{A}|i\rangle, \quad (1)$$

is approximately written as

$$M_{if} \approx (e/mc\hbar\omega)\vec{A}\cdot\langle f|\nabla V|i\rangle, \quad (2)$$

as in Refs. 6–8: (1) For oblique incidence, $\theta_i \neq 0$, the optical field is not a pure transverse wave but has a longitudinal A_z component due to the induced-polarization charge ρ_s, given by

$$\langle\nabla\cdot\vec{A}\rangle_{z=0} = (4\pi ic/\omega)\rho_s. \quad (3)$$

(2) The spatial variation of the optical field need not contain the same Fourier components as the incident wave but can exhibit strong nonlocal effects[9] so that the field cannot be replaced in Eq. (1) with its macroscopic average shown in Fig. 3(a). A detailed quantitative calculation is outside the scope of this paper. However, we have shown that the commonly accepted simple connection between orbital symmetry[6-8] (i.e., potential gradients) and photon polarization is not possible without considering the strong E_z effects due to the dielectric properties of the solid.

Helpful discussions with D. E. Aspnes, J. A. Appelbaum, D. R. Hamann, J. C. Phillips, and M. M. Traum are gratefully acknowledged as well as the experimental assistance of S. B. Christman.

[1]H. E. Ives and H. B. Briggs, Phys. Rev. 38, 1477 (1931); D. W. Juenker, J. P. Waldron, and R. J. Jaccodine, J. Opt. Soc. Amer. 54, 216 (1964); R. M. Broudy, Phys. Rev. B 3, 3641 (1971); M. S. Jazzar and T. E. Fischer, Surface Sci. 42, 565 (1974).

[2]K. Mitchell, Proc. Roy. Soc., Ser. A 146, 442 (1934).

[3]J. G. Endriz and W. E. Spicer, Phys. Rev. B 4, 4144 (1971); P. O. Gartland, S. Berge, and B. J. Slagsvold, Phys. Rev. Lett. 30, 916 (1973).

[4]J. G. Endriz, Phys. Rev. B 7, 3464 (1973).

[5]S. A. Flodström and J. G. Endriz, Phys. Rev. Lett. 31, 893 (1973).

[6]V. Heine, in *Proceedings of the Tenth International Conference on the Physics of Semiconductors, Cambridge, Massachusetts, 1970,* edited by S. P. Keller, J. C. Hensel, and F. Stern, CONF-700801 (U.S. AEC

Division of Technical Information, Springfield, Va., 1970), p. 228.
[7]G. D. Mahan, Phys. Rev. B 2, 4334 (1970); A. Liebsch, Phys. Rev. Lett. 32, 1203 (1974).
[8]H. D. Hagstrum and G. E. Becker, Proc. Roy. Soc., Ser. A 331, 395 (1972).
[9]K. L. Kliewer, Phys. Rev. Lett. 33, 900 (1974).
[10]J. E. Rowe, S. B. Christman, and E. E. Chaban, Rev. Sci. Instrum. 44, 1675 (1973).
[11]J. E. Rowe, H. Ibach, and H. Froitzheim, to be published; H. Ibach and J. E. Rowe, Surface Sci. 43, 481 (1974).
[12]W. D. Grobman and D. E. Eastman, Phys. Rev. Lett. 29, 1508 (1972); D. E. Eastman and W. D. Grobman, Phys. Rev. Lett. 28, 1378 (1972).
[13]W. N. Hansen, J. Opt. Soc. Amer. 63, 1131 (1973).
[14]The calculated maximum is somewhat dependent on values of optical constants assumed: E. T. Arakawa, R. N. Hamm, and M. W. Williams, J. Opt. Soc. Amer. 63, 1131 (1973).
[15]B. Feuerbacher and B. Fitton, Solid State Commun. 15, 295 (1974).
[16]J. A. Appelbaum and D. R. Hamann, Phys. Rev. Lett. 32, 225 (1974).

Parity Mixing in ^{19}F†

E. G. Adelberger,* H. E. Swanson,‡ M. D. Cooper, J. W. Tape,§ and T. A. Trainor
Department of Physics, University of Washington, Seattle, Washington 98195
(Received 5 November 1974)

The parity-nonconserving asymmetry of the 110-keV de-excitation radiation emitted by a polarized ensemble of ^{19}F nuclei in the first excited state is found to be $\delta = -(1.8 \pm 0.9) \times 10^{-4}$.

The study of parity-nonconserving (PN) nucleon-nucleon forces provides a unique opportunity to observe the weak hadronic current interacting with itself.[1,2] At present most experimental evidence for the size of parity admixtures in nuclear states comes from circular polarization (CP) measurements in heavy nuclei. In these nuclei the complexities of the nuclear structure tend to obscure the properties of the basic PN interaction. It is, therefore, highly desirable to study parity mixing in light nuclei where the nuclear physics is relatively tractable and where one can elucidate the isospin structure of the PN forces.

Prior to this work there existed only two positive measurements of PN transitions in light nuclei—a CP measurement of the radiation from capture of thermal neutrons by hydrogen[3] and a measurement[4] of the PN α decay of the 8.8-MeV 2^- level of ^{16}O. The α-decay width in ^{16}O is roughly in accord with theory, while the CP measurement in H(n,γ) is about 100 times larger than expected with current theories.[2] The apparent strong discrepancy between these two examples is not understood.

We have measured parity mixing in the ground ($J^\pi = \frac{1}{2}^+$) and 110-keV ($J^\pi = \frac{1}{2}^-$) excited states of ^{19}F. In this instance the nuclear physics is unusually simple but unlike the cases of ^{16}O and $p+n$ which are sensitive only to the $\Delta I = 0$ or $\Delta I = 2$ PN interactions,[1,2] the $\Delta I = 1$ PN interaction is also involved. It is particularly interesting to study the $\Delta I = 1$ interaction since it may be sensitive to neutral weak currents. The mixing in ^{19}F is well approximated by simple two-state theory because the next $J = \frac{1}{2}$ level occurs at $E_x = 5.34$ MeV and the irregular transition is $M1$.[5] Since the PN interaction is a small perturbation we have

$$|\text{g.s.}\rangle = |+\rangle - \epsilon|-\rangle,$$

$$|110\rangle = |-\rangle + \epsilon|+\rangle,$$

where $\epsilon = \langle - |H_{\text{PN}}| + \rangle / (110\ \text{keV})$. The electromagnetic matrix element connecting the states contains regular ($E1$) and irregular ($M1$) components:

$$\langle \text{g.s.}|E1+M1|110\rangle = \langle +|E1|-\rangle + \epsilon[\langle +|M1|+\rangle - \langle -|M1|-\rangle] + O(\epsilon^2),$$

where we have ignored PN exchange contributions. The PN $M1$ amplitudes are completely determined by ϵ and the magnetic moments of the $\frac{1}{2}^+$ and $\frac{1}{2}^-$ levels. Our experiment measures ϵ by detecting the $M1$-$E1$ interference which produces a pseudoscalar anisotropy $\sigma(\theta) = \sigma_0(1 + \delta \vec{P}_F \cdot \vec{k}_\gamma)$ in the 110-keV de-excitation radiation from a polarized ensemble of ^{19}F* ($\vec{P}_F$ represents the ^{19}F* polarization vector and $\vec{k}_\gamma$ a unit vector along the γ-